Proc. Annual Meeting of the Austrian Society for Biomedical Engineering 2021
DOI: 10.3217/978-3-85125-826-4-09

OPTIMIZATION OF PULSED CHEMICAL EXCHANGE SATURATION TRANSFER MRI BY OPTIMAL CONTROL

Clemens Stilianu[1], Christina Graf[1], Armin Rund[2], Rudolf Stollberger[1]

[1]Institute of Medical Engineering, Graz University of Technology, Graz, Austria
[2]Institute for Mathematics and Scientific Computing, University of Graz, Graz, Austria

stilianu@tugraz.at

Abstract— *The goal of this work was to design improved Chemical Exchange Saturation Transfer MRI RF pulses applicable to whole-body clinical scanners. Conventionally, CEST imaging requires a long continuous wave saturation pulse, however, due to hardware limitations, only pulsed saturation is practicable for in vivo scanners. Consequently, RF pulses with a duty cycle of 90% are designed by optimal control. The simulation results were compared to a 100% duty cycle Continuous-Wave pulse and a 90% Gaussian standard pulse. The optimal control pulse showed superior efficiency to the Gaussian pulse and comparable performance to the Continuous-Wave pulse, while transmitting less energy to the patient.*

Keywords—*CEST, Pulsed CEST MRI, Optimal Control, Optimization, Pulse Design*

Introduction

Chemical Exchange Saturation Transfer (CEST)-MRI is a specific imaging method that can efficiently detect various metabolites in the human body undetectable by conventional MRI [1]. This can be realized by applying a long, off-resonant Continuous Wave (CW) saturation radio frequency (RF) pulse. However, such pulses are not always feasible due to hardware limitations and Specific Absorption Rate (SAR) restrictions, especially on clinical scanners which require pulsed RF excitation which typically provide much lower saturation, [1]. Optimal Control (OC) is emerging as a promising tool to find Duty Cycled (DC) pulses that achieve high CEST-effects while accounting for hardware limitations of clinical scanners. OC CEST pulses with a DC of up to 90% are designed to challenge CW pulses and exceed state of the art pulses used on clinical scanners.

Theory and Methods

Bloch-McConnell equations are the basis for describing chemical exchange phenomena in MRI. Explicitly, they describe a six-dimensional inhomogeneous system of ODEs giving us the temporal evaluation of the magnetization vector $M(z,t)$:

$$\frac{dM}{dt} = A \cdot M + b, \qquad \frac{d\tilde{M}}{dt} = \tilde{A} \cdot \tilde{M} + b,$$

$$s.t. \quad M(t=0) = M_0, \qquad \tilde{M}(t=0) = \tilde{M}_0. \tag{1}$$

The Bloch-McConnell equations in this case include two proton pools, one pool for bulk water and one pool for the solute, which are connected via chemical exchange with exchange rate k_{sw} from solute pool to bulk water pool and exchange rate k_{ws} from the bulk water pool to the solute pool. Therein, M and A describe the system with chemical exchange and $\tilde{\mathrm{M}}$ and $\tilde{A}$ describe the system without chemical exchange. Each of the pools are defined individually by relaxation times T_{1w} and T_{2w} for bulk water and T_{1s} and T_{2s} for the solute pool.

The optimization problem is given as

$$\min_{B_1} J\left(B_1, M_z, \tilde{M}_z\right) = \frac{\alpha}{2}\int_0^T (B_1)^2\, dt - \\ -\beta\left|M_z(z_1) - \tilde{M}_z(z_1)\right| - \gamma \int_\Omega \mathrm{M}_z(z)\, dz. \tag{2}$$

The first integral of Eq. 2 corresponds to the transmitted energy in the B_1 field with the regularization parameter α. The second term maximizes the difference between the magnetization M_z with CEST and the magnetization $\tilde{M}_z$ without CEST at the saturation offset z_1, i.e. maximization of the corresponding CEST peak weighted with parameter β. The third term ensures the maximization of the area under the z-spectrum by integrating over the whole frequency space Ω weighted by the parameter γ. The design of this cost function was inspired by [2].

For OC, the DC of the RF-pulse is fixed to a value of 90% with an on time of $t_p = 100$ ms and subsequent off times of $t_d = 12.5$ ms (see Tab. 2). 90% DC is chosen to maximize the on time and therefore the dependent CEST effect as well as ensure the feasibility of measurements on clinical MRI scanners. For performance review, the simulation is also conducted for a CW pulse with a DC of 100% and a Gaussian standard pulse with the same t_p and t_d times as the OC pulse. The Gaussian standard pulse is a Gaussian function filtered with a cosine window which is directly taken from [3]. The amplitude of the CW pulse as well as the Gaussian standard pulse is optimized to yield a maximum CEST effect for this model, thus the best CW pulse and Gaussian standard pulse for a given saturation time are used within the following comparison.

Published by Verlag der TU Graz
Graz University of Technology

DOI: 10.3217/978-3-85125-826-4-09

The simulation and optimization process is demonstrated using the example of a creatine pool with a frequency offset of $\delta = 1.9$ ppm in chemical exchange with a bulk water pool with no offset (see Tab. 1). The simulation parameters are taken from [4].

Table 1: Simulation parameters for the creatine CEST model including a water pool and a solute pool.

Simulation Parameter	**Value**
Offset, δ [ppm]	1.9
Exchange rate solid-water , k_{sw} [Hz]	50
Exchange rate water-solid , k_{ws} [Hz]	1
B_0 [T]	3
Relaxation, T_{1w} [s]	1.08
Relaxation, T_{2w} [ms]	0.069
Relaxation, T_{1s} [s]	1.00
Relaxation, T_{2s} [ms]	0.160
Time discretization, Δt [ms]	0.1
Frequency discretization, Δz [ppm]	0.05

The RF pulse is optimized with a hybrid semismooth quasi-Newton method [5] which also allows the implementation of constraints prescribed by the clinical scanner (Amplitude: $B_{1max} \leq 2.5\ \mu T$ and Phase: $0 \leq \varphi \leq 2\pi$). The underlying Bloch-McConnell equations and their corresponding adjoint equations are solved numerically by symmetric operator splitting [6].

Results and Discussion

The optimized pulse can be seen in Fig. 2 on the top right and the corresponding spectrum underneath.

There, the saturated spectrum without exchange $\widetilde{M}(z)$

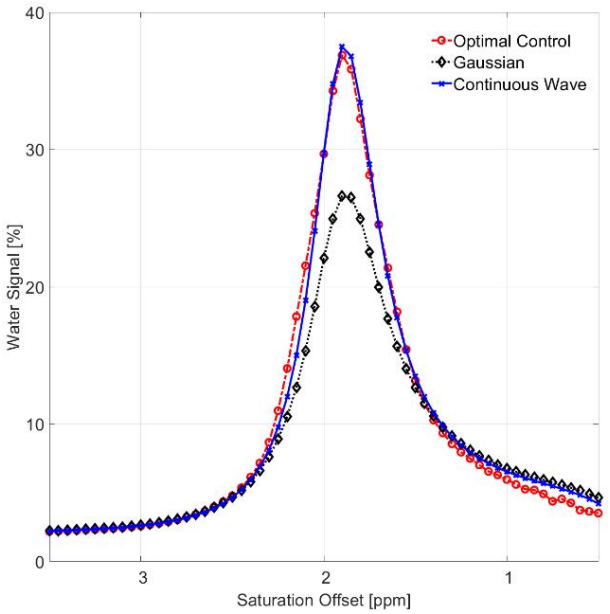

Figure 1 : Direct comparison of the CEST-Peaks for the CW- , OC- and Gaussian-pulse.

is shown in blue, the one with chemical exchange $M_z(z)$ in red, and the CEST effect is seen as difference $|M_z(z) - \widetilde{M}_z(z)|$. To compare the performance of the OC results the same model is tested with a CW pulse and a Gaussian standard pulse. CW pulses are broadly known as the most efficient pulses for generating high contrast CEST images, mainly used for NMR spectroscopic measurements. However these pulses are not applicable on clinical scanners due to

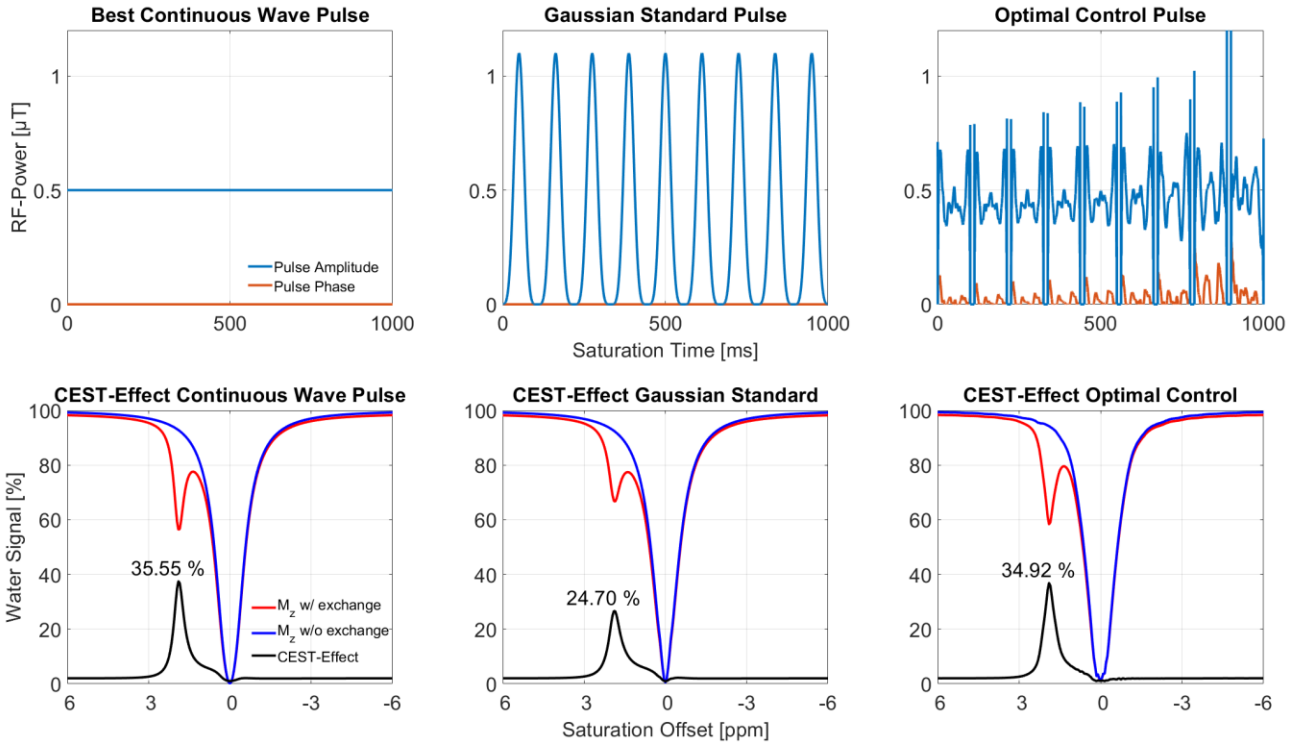

Figure 2: Comparison of the CW- , OC- and Gaussian-pulses and the corresponding z-spectra.

Published by Verlag der TU Graz
Graz University of Technology

DOI: 10.3217/978-3-85125-826-4-09

hardware limitations and SAR restrictions. That is why pulsed Gaussian standard pulses or pulsed truncated sinc pulses (not included in this work) are currently used as most efficient RF pulses for CEST imaging.

By comparing the spectra that are generated with the OC, CW and Gaussian pulses we can get an understanding of how efficient the pulses generate contrast in CEST images. Smooth and slim spectra potentially generate easy to distinguish CEST peaks for measurements. Therefore, minimizing the negative integral is a priority for the optimization process, as this on the one hand limits the energy that is put into the RF pulse, and on the other hand restrains broadening of the CEST peak and truncates artefacts in the resulting spectra. All pulses exhibit a comparatively small area as can be seen in Tab. 2. The CEST peaks of all pulses can be seen in greater detail in Fig. 1. The CEST peak maximum of the OC pulse reaches the CEST peak maximum of the CW within approximately 1.7 % and beats the maximum of the Gaussian pulse by about 30.5 %.

Furthermore, a restriction to a MRI RF pulse is the energy transferred to the human's body. The Integral of $(B_1(t))^2$ over the pulse duration is proportional to said energy, hence proportional to the SAR [7]. In Tab. 2 we observe that the Gaussian RF pulse train exhibits the highest energy, followed by the CW with OC showing the lowest energy among those three. This underlines that OC addresses those limitations successfully.

The presented RF pulse designed by means of optimal control showed to outperform state of the art pulses in terms of CEST effect and pulse energy. The next logical step would be the implementation on the MR scanner and comparison to both the CW and Gaussian RF pulse.

Table 2: Comparison of significant features of a CW pulse with a DC-OC pulse and a DC-Gaussian standard pulse. Total duration was set to 1 s.

Pulse feature	**CW**	**Gaussian**	**OC**
CEST-Effect [%]	35.55	24.70	34.94
Integral $(B_1(t))^2$ [(µT)^{2}s]	2500	2844	2094
Area [a.u.]	200	191	198
Duty Cycle, DC [%]	100	90	90

Conclusion

We implemented an optimal control framework for CEST RF pulse design. The optimized pulses were able to outperform state of the art Gaussian pulses by 30.5% and achieve almost the same efficiency as CW pulses while being applicable to clinical scanners.

References

[1] S. A. Smith, J. A. D. Farrell, C. K. Jones, D. S. Reich, P. A. Calabresi, and P. C. M. Van Zijl, "Pulsed magnetization transfer imaging with body coil transmission at 3 Tesla: Feasibility and application," *Magn. Reson. Med.*, vol. 56, no. 4, pp. 866–875, Oct. 2006, doi: 10.1002/mrm.21035.

[2] E. S. Yoshimaru, E. A. Randtke, M. D. Pagel, and J. Cárdenas-Rodríguez, "Design and optimization of pulsed Chemical Exchange Saturation Transfer MRI using a multiobjective genetic algorithm," *J. Magn. Reson.*, vol. 263, pp. 184–192, Feb. 2016, doi: 10.1016/j.jmr.2015.11.006.

[3] K. Herz *et al.*, "Pulseq-CEST: Towards multi-site multi-vendor compatibility and reproducibility of CEST experiments using an open-source sequence standard," *Magn. Reson. Med.*, vol. 00, pp. 1–14, 2021, doi: 10.1002/mrm.28825.

[4] M. Zaiß, B. Schmitt, and P. Bachert, "Quantitative separation of CEST effect from magnetization transfer and spillover effects by Lorentzian-line-fit analysis of z-spectra," *J. Magn. Reson.*, vol. 211, no. 2, pp. 149–155, Aug. 2011, doi: 10.1016/j.jmr.2011.05.001.

[5] A. Rund, C. S. Aigner, K. Kunisch, and R. Stollberger, "Magnetic Resonance RF Pulse Design by Optimal Control with Physical Constraints," *IEEE Trans. Med. Imaging*, vol. 37, no. 2, pp. 461–472, Feb. 2018, doi: 10.1109/TMI.2017.2758391.

[6] C. Graf, A. Rund, C. S. Aigner, and R. Stollberger, "Accuracy and Performance Analysis for Bloch and Bloch-McConnell Simulation Methods," *J. Magn. Reson.*, p. 107011, May 2021, doi: 10.1016/j.jmr.2021.107011.

[7] M. A. BERNSTEIN, K. F. KING, and X. J. ZHOU, "INTRODUCTION TO RADIOFREQUENCY PULSES," in *Handbook of MRI Pulse Sequences*, Elsevier, 2004, pp. 29–34.

Published by Verlag der TU Graz
Graz University of Technology